Eng. Sci., 2025, **37**, 1831

Engineered Science
DOI: https://dx.doi.org/10.30919/es1831

Electrical Output Simulation Model for a Photovoltaic Microgrid

Guang Yu, Lijie Peng and Yujia Cheng*

Abstract

With the global energy mix transformation, new energy resources, particularly luminous energy, have garnered increasing attention, along with a gradual increase in their proportion in the electric power sector. However, challenges in new energy resource consumption and system planning persist. Therefore, this study develops a power supply planning model based on a photovoltaic (PV) microgrid system. This model can be applied to improve the consumptive ability of new energy resources, optimize the power combination, and realize the sustainable development of the power system. System modeling and simulation analysis are conducted using MATLAB/Simulink software to analyze the electrical output characteristics for PV microgrid system optimization. PV power and direct current load models are initially established, and the effects of different parameters on the power curves are analyzed. The results demonstrate that the developed mathematical models are effective in simulating the electrical output characteristics of PV microgrid systems. Additionally, the model optimizes the power supply, supporting the sustainable development of the power system. Adjusting the model parameters significantly influences the system output, which is valuable for designing and optimizing PV power generation systems.

Keywords: Photovoltaic direct current microgrid; Power output; Simulation model; Output characteristics.
Received: 27 July 2025; Revised: 12 October 2025; Accepted: 22 October 2025
Article type: Research article.

1. Introduction

With the rapid depletion of fossil fuels, there has been growing interest in the development of renewable energy sources. New energy resources, such as solar, wind, hydro, geothermal, and bioenergy are garnering significant attention.[1] Among this luminous energy is a critical component owing to its minimal environmental impact. The energy conversion process produces almost no pollutants and requires no additional resources compared with traditional fossil fuels, making it environmental friendly.[2] With advancement in photovoltaic (PV) technology, the construction and operation of PV power generation systems have become significant drivers of economic growth. In the late 20th century, scientific researchers discovered the phenomenon of the PV effect, where sunlight illuminating the surface of semiconductor materials generates an induced current.[3] Technological advancement has led to the successful development of monocrystalline Si solar cells, making a breakthrough in solar-to-energy conversion.[4] In Europe, United States and Japan, the microgrids basic theoretical analysis is completed. The model tools and simulation tools of distributed energy resources and microgrids are preliminary establishment.[5] According to the verification of experimental test and on-side demonstration, the basic theory of microgrids operation, protection and economic analysis can be solved. The available microgrid models are mainly built based on microgrids economic operation. However, the microgrid models combined with renewable energy and energy storage are missing, from which the important role of renewable energy on microgrid operation is unable to reflect.[6] Therefore, in this manuscript, a microgrid model based on renewable energy is proposed. This model is developed in Matlab, from which the output characteristic of PV microgrid can be observed directly.

In traditional energy systems, distribution networks primarily use alternating current (AC).[7] However, recent studies have proposed a direct current (DC) microgrid to reduce energy conversion loss in transmission systems. This approach reduces power and DC load conversion losses, enhancing economic efficiency. It also avoids synchronization with large AC power grids.[8] For security, the bus voltage remains stable during power outages or voltage drops owing to the high energy storage capacity of the DC capacitor and converter voltage control.[9] A comprehensive cost estimation comparison of DC and AC microgrids is shown in Table 1.[10] This study presents a power supply planning mathematical model based on a photovoltaic (PV) microgrid system.

PV power generation is essential for the development and application of solar energy and is reliant on PV cells.[11] Due

Mechanical and Electrical Engineering Institute, University of Electronic Science and Technology of China, Zhongshan Institute, Zhongshan, 528400, China
*Email: chengyujia@zsc.edu.cn (Yujia Cheng)

Table 1: Comprehensive cost estimation comparison of DC and AC microgrids.

Cost item	AC microgrid	DC microgrid	Comparison
PV module	Identical	Identical	No difference
Inverter	High (DC-AC)	Low (DC-DC)	DC system is cheaper in the DC environment
Energy storage system	High (AC-DC)	Low (DC)	High DC storage efficiency
Power distribution equipment	Medium	Low (Low pressure)	High cost of high voltage DC switch
Harmonic control	High (Active power filter)	None	AC system requires an additional filter
Running loss	Higher	Low	Less DC conversion
Maintenance cost	Higher	Low	Simple maintenance for DC equipment
Load compatibility	High (Conventional loading)	Low (Reconstruction)	Special-purpose load for DC system

to their parameters, ambient temperature, illuminance, and loads, the electrical output characteristics of PV cells are nonlinear. To effectively improve PV power generation system efficiency, a maximum power point tracking (MPPT) control device is commonly used, including a PV array module, MPPT algorithm, pulse width modulation (PWM) module, and DC/DC transformation module. Among them, the PV array module is formed by multiple PV cell units in series and parallel connections with tight packing. The MPPT module mainly includes the control algorithm. There is currently a wide variety of MPPT algorithms,[12] each with their own advantages and limitations. Owing to its mature development, simple control, and high precision, the perturbation and observation method and incremental conductance (INC) are used commonly. The PWM module output is used as the drive signal of DC/DC circuits. In DC/DC conversion, buck and boost converters have the highest efficiencies. For a buck converter, the high voltage can be transformed to low voltage. In general, the output voltage level of a PV array is low.[13] Therefore, a buck converter is seldom used the grid-connected process, as the grid-side level must be higher. For a boost converter, the output voltage of the PV array increases, making the grid-connected process easy to implement. Furthermore, the impedance transformation function of a boost converter is commonly used for MPPT control as the circuit is easily driven.

In this study, based on the analysis of an MPPT control model in PV power generation, Simulink models for different modules are built. Among them, the PV cell model is built using an engineering mathematics model. The MPPT algorithm uses the INC method and the boost converter is used for DC/DC conversion. Based on an analysis of these modules, the MPPT control system based on a boost circuit is explored in detail. Furthermore, this approach can also be applied to analyze MPPT control in actual PV power generation systems.

2. Simulation of a PV microgrid

The primary modules of PV microgrid include a PV cell, boost converter, and DC load. This system forms a compact microgrid model, as illustrated in Fig. 1.

2.1 PV cell modeling

The system current was determined by the output power of the PV array. The output current of the solar cell was calculated as follows:

$$I=I_p-I_v\left\{\exp\left[\frac{q(V+IR_x)}{AKT}\right]-1\right\}-\frac{V+IR_s}{R_{SH}} \quad (1)$$

where I_p is the photocurrent; I_0 is the diode saturation current; E_α is the Mittag-Leffler function; α is the degree of fractional order; A is the diode quality factor; q is the charge constant; K is the Boltzmann constant; T is the PV cell temperature; and R_S and R_{SH} are the internal resistances of the PV cell in series and parallel connections, respectively.[14]

To accurately calculate the output current, the relevant parameters were adjusted to simplify Eq. (1), as follows:

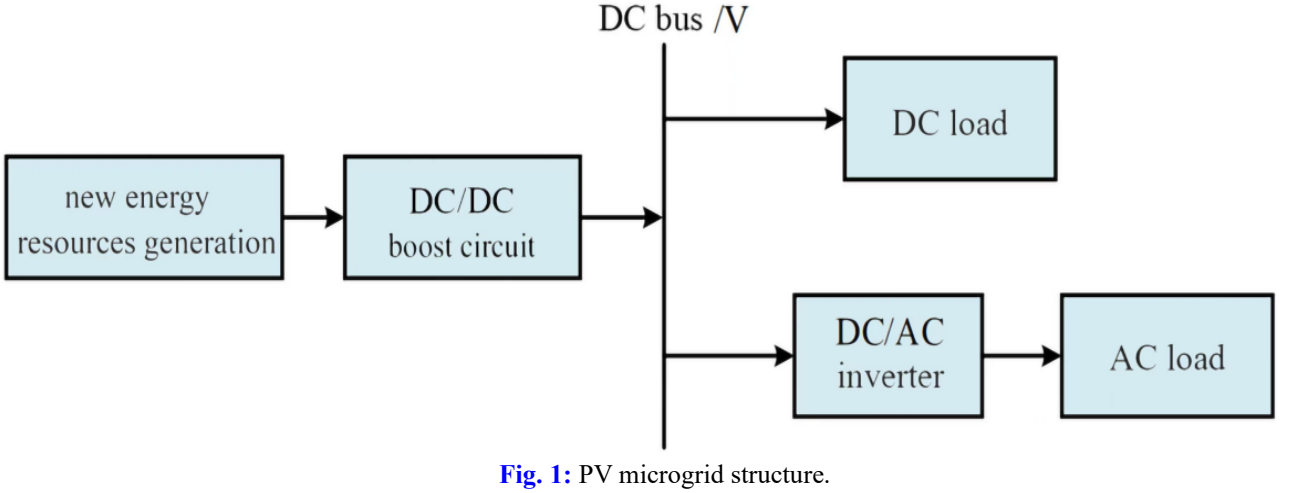

Fig. 1: PV microgrid structure.

$$I=I_{sc}-\left[1-A\left(e^{\frac{U}{BU_{oc}}}-1\right)\right] \quad (2)$$

For simplicity, Eq. (2) was rewritten as follows:

$$I_m=I_{sc}-\left[1-A\left(e^{\frac{U_m}{BU_{oc}}}-1\right)\right] \quad (3)$$

where B represents the battery capacity.

To simplify the calculation at room temperature, the value of $\frac{eU_m}{BU_{oc}}$ exceeded one, as follows:

$$I_m = I_{sc}\left(1-\frac{I_m}{I_{sc}}\right)e^{\frac{-U_m}{BU_{oc}}} \quad (4)$$

The state of the electric circuit was precisely represented as follows:

$$I_S = I_{sc}\left[1-\left(1-\frac{I_m}{I_{sc}}\right)e^{\frac{-U_m}{BU_{oc}}}\left(e^{\frac{1}{B}}-1\right)\right] \quad (5)$$

when $e^{\frac{1}{B}}$ significantly exceeded one, the battery capacity was as follows:

$$B = \left(\frac{U_m}{U_{oc}}-1\right)\left[I_n\left(1-\frac{I_m}{I_{sc}}\right)\right]^{-1} \quad (6)$$

Eq. (2) - (6) were incorporated into a simulation model, from which the voltage–current (U-I) characteristic curve of the PV power was obtained.[15]

After obtaining the U-I characteristics, the values of the light intensity and system temperature variation were calculated.[16] Subsequently, these values were substituted into Eq. (7) - (11) and used in the simulation. Firstly, the model was used to simulate normal external conditions (solar external condition $S_{ref} = 1000\,w/m^2$ and ambient temperature $T_{ref} = 25°C$). The power-voltage (P-V) simulation curves before and after MPPT tracking were then obtained.

$$\Delta t = t = t_{ref} \quad (7)$$

$$I'_{OC} = I'_{SC}\left(\frac{s}{s_{ref}}\right)(1+\alpha\Delta t) \quad (8)$$

$$\Delta s = \frac{s}{s_{ref}} - 1 \quad (9)$$

$$I'_m = I_m\left(\frac{s}{s_{ref}}\right)(1+\alpha\Delta t) \quad (10)$$

$$U'_m = U_m(1-c\Delta t)(1+b\Delta s) \quad (11)$$

The PV power simulation model was developed using MATLAB/Simulink simulation software, as shown in Fig. 2,[17] where f(u) is the S-function and the S-function module represents the s-function of MPPT in the PV module.

2.2 DC load modeling

Compared with PV power, establishing a DC load model is more convenient. The resistive-inductive-capacitive (RLC) load was selected using the Simscape module.

The selected components were loaded into the simulation model. After encapsulation, a DC pulse load was obtained.[18] These load power variations were processed using module instructions that possessed good flexibility and operation. This model is shown in Fig. 3.

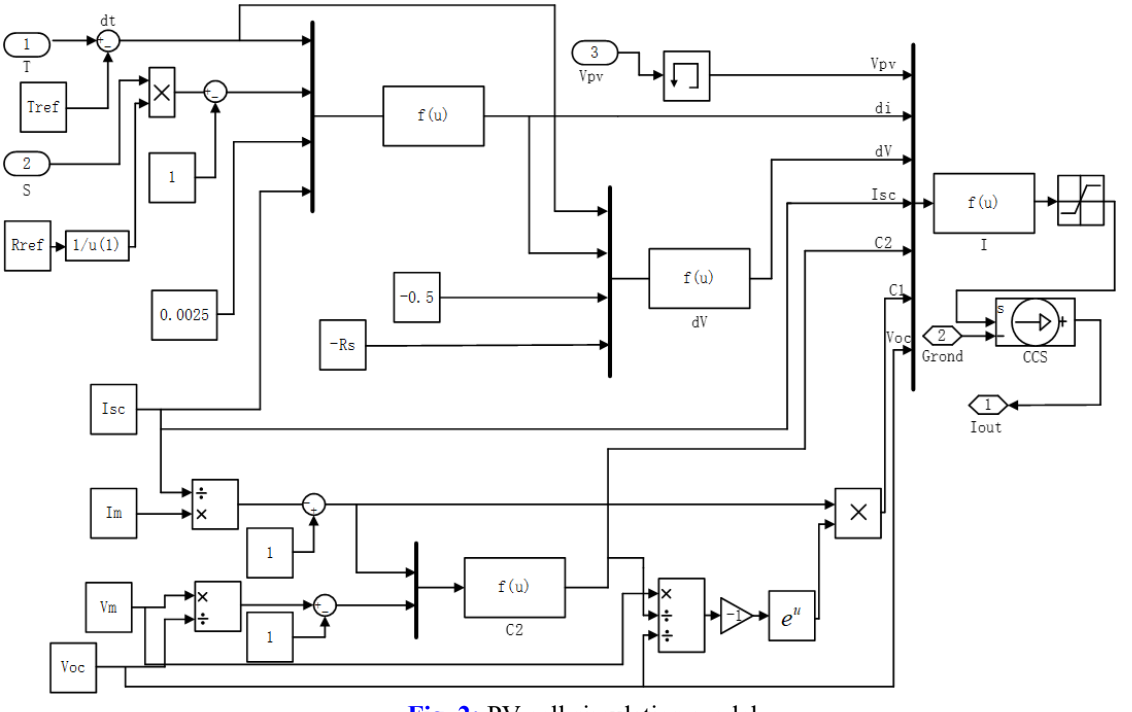

Fig. 2: PV cell simulation model.

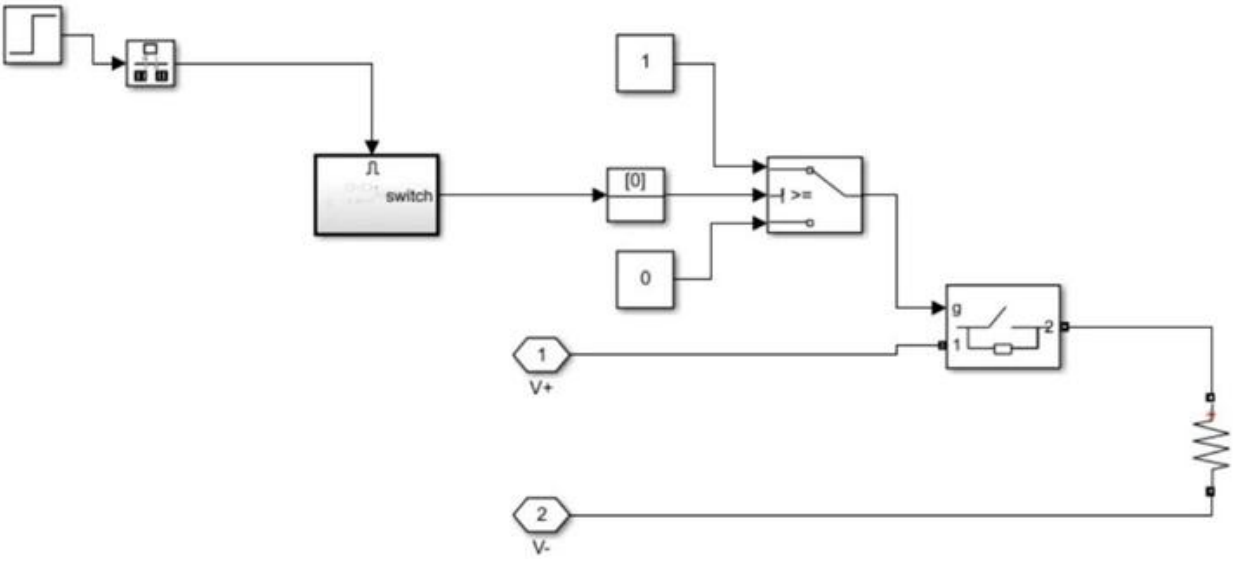

Fig. 3: DC load system model.

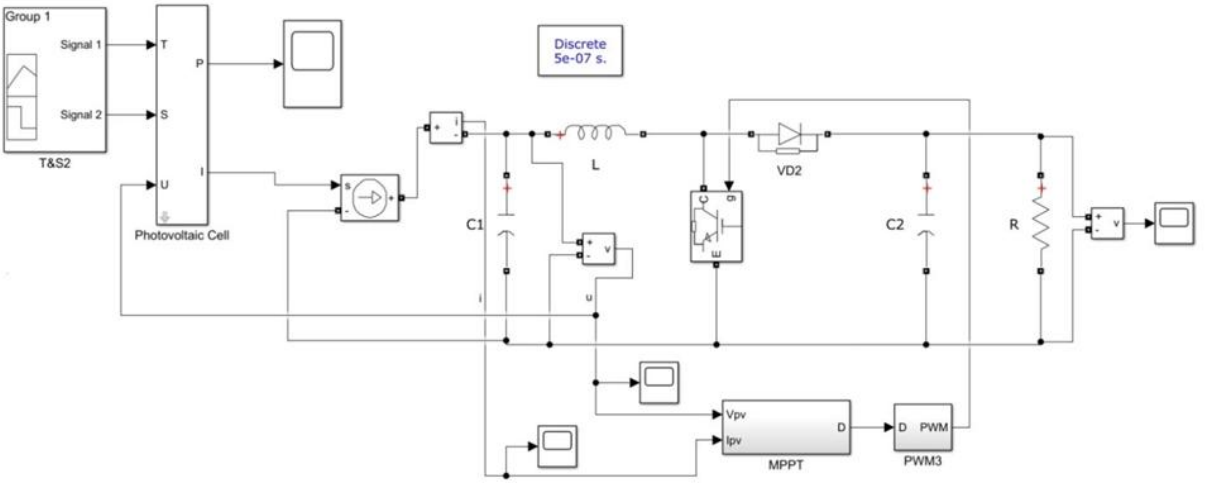

Fig. 4: PV microgrid simulation model.

2.3 DC microgrid modeling and parameter settings

After modeling each module, a DC microgrid simulation model was built using Simulink software, as shown in Fig. 4.[19] The elapsed time was set as 3 s, while the discrete step was set at 5×10^{-7} s.

The simulation environment was set as a discrete state, and the ode23tb simulation algorithm was used. Other simulation parameter settings included the maximum and minimum step sizes.

The important parameters of each simulation component are listed in Table 2. The reference standard was IEC 61850-7-420: Distributed energy resources (including PV) communication and automation.[20]

3. System simulation results and analysis

3.1 Output characteristic analysis of the PV cell

The P-V characteristics of the PV array are shown in Fig. 5. When the operating voltage of the generator was lower than the maximum voltage *Vmax*, the output voltage of the PV array increased.[21–23] However, when the operating voltage exceeded *Vmax*, the output voltage gradually decreased, leading to a reduced output power of the PV array.[24,25] From the curve graph, the PV array performance can be optimized automatically using MPPT technology.[26] According to the voltage regulation on the console, the output power of the PV array can be adjusted under varying temperatures and lighting conditions, which improves the efficiency.

Table 2: Model parameters.

Name	Numerical value
Stabil Volt capacitor in PV side/F	$20e^{-5}$
Filter inductance in PV side/H	$300e^{-6}$
DC load/Ω	30
Capacitor in load side/F	$100e^{-6}$

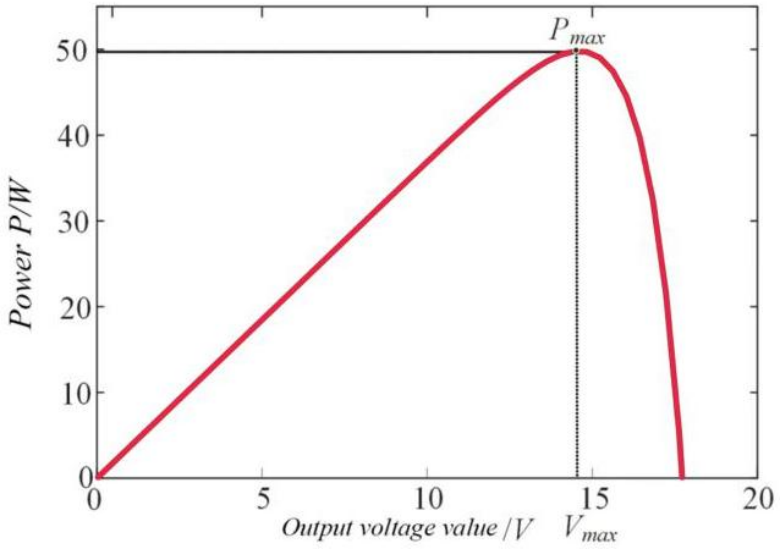

Fig. 5: P-V characteristic curve of the PV array.

Studies have demonstrated that fluctuations in temperature and light intensity continuously affect the output power, no-load voltage, and short-circuit current of PV arrays. These environmental changes alter the equilibrium points of the system, reducing efficiency and impacting the rate of energy conversion, which is shown in Fig. 6. Therefore, the adaptability of the system to environmental changes must be improved.[27,28] Power variation under different situations must be constantly monitored to maintain maximum power output (MPO). Therefore, a detailed system-control strategy must be explored. Consequently, the output characteristics of the PV cell were analyzed.

(1) I/U and P/U characteristic curves under a constant temperature and different light intensities:

The operating temperature of the PV unit was set a constant 25 ℃. The simulations of the effects of different light intensities on the PV array are shown in Fig. 7.

From Fig. 7(a), under a constant ambient temperature (25 ℃), the battery current increased with increasing light intensity. Additionally, the open-circuit voltage (OCV) slightly increased, but its growth rate was lower than that of the electric current. This indicates that electric voltage is less sensitive to changes in illumination.[29,30] A single parabolic peak was observed in the P-U characteristic diagram. At 25 ℃, the battery output power positively correlated with light intensity, but beyond the maximum power point (MPP), the system power decreased despite an increase in voltage. In Fig. 7(b), the MPP was also positively correlated with light intensity. Therefore, under constant ambient temperature, the output power of the PV module positively correlates with light intensity.

(2) I/U and P/U characteristic curves for a constant light intensity and different temperatures:

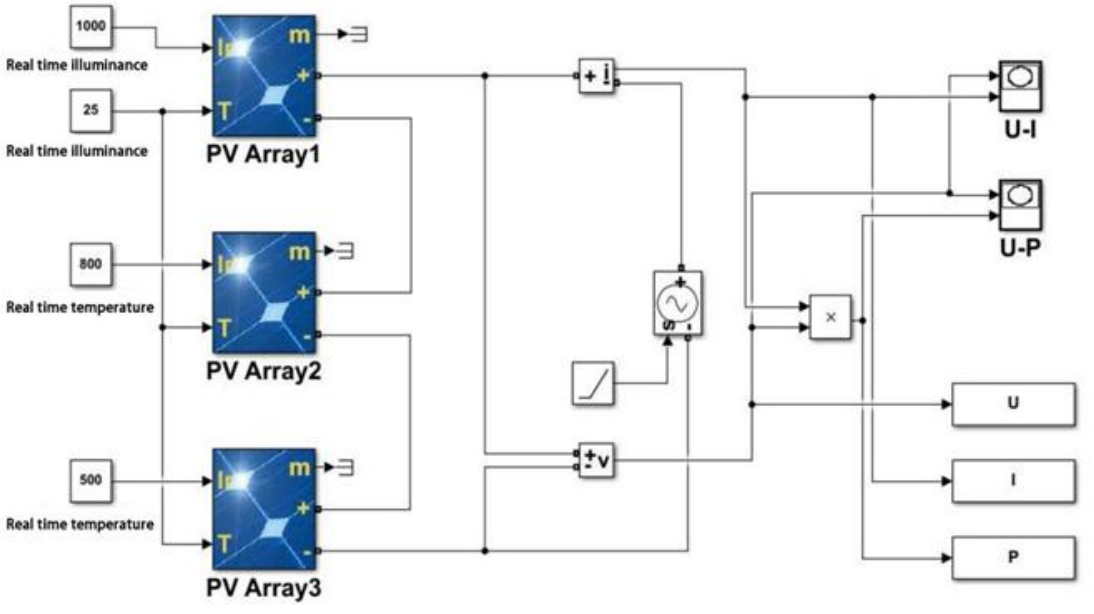

Fig. 6: Real-time tracking power in different working conditions.

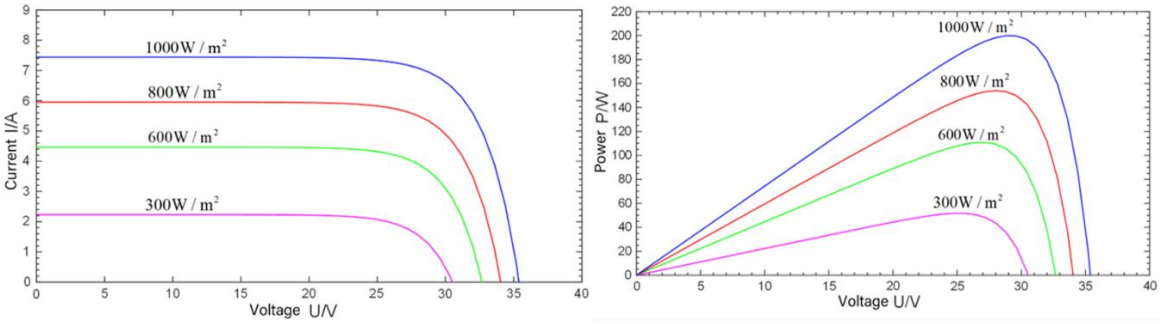

(a) I/U characteristic curves for different light intensities. (b) P/U characteristic curves at different light intensities.

Fig. 7: I/U (a) and P/U (b) characteristic curves of different light intensities at a constant temperature.

Subsequently, the light intensity of the PV unit was set to a constant 1000 W/m^2. The simulations of the effects of different temperatures on the PV array are shown in Fig. 8.

As shown in Fig. 8(a), with increasing temperature, the electric voltage decreased as the electric current increased. This change was more significant at different temperatures. Fig. 8(b) shows that the temperature increased with decreasing output power, which explains the inverse proportionality between the maximum power and temperature. Consequently, under constant light conditions, an increase in temperature caused the output photovoltaic (OPV) device voltage to decrease while increasing the current, ultimately reducing the output power. By contrast, when the temperature decreased, the property parameters of the PV device exhibited a reverse trend. The experimental result is consistent with the IEC 61850-7-420 standard. The error bound from the comparison of the simulation results with the partial differential equation (PDE) analytical solution was obtained as

$\|P_{sim} - P_{mod\,el}\| < 5\%$.

According to the PV characteristic curves, the relationship between the voltage and current of the PV cell is completely different to that of a traditional energy storage cell. As the voltage increased, the current decreased. From the product of the voltage and current, the power change curve caused by the voltage was obtained. As the voltage increased, the power first increased and then decreased; therefore, an MPP existed. To improve the efficiency of the PV cell, it should always operate in MPPT. Therefore, research on the MPPT tracking algorithm in PV cells is extremely important.[31]

3.2 Calculation process of the maximum power algorithm

The maximum power algorithm significantly affects the electrical output characteristics. Variations in temperature and light intensity can affect the MPP of a PV cell, as well as its output voltage and current. In DC/DC conversion, buck and boost converters have the highest efficiencies. For a buck converter, the high voltage can be transformed to a low voltage. In general, the output voltage level of a PV array is low. For the grid-connected process, the grid-side level must be higher; therefore, a buck converter is seldom used. For a boost converter, the output voltage of the PV array increases, making the grid-connected process easy to implement. In addition, the impedance transformation function of a boost converter is commonly used for MPPT control and the circuit is easily driven.

The boosting process of a DC boost circuit is the energy transfer process of inductance. On charge, the inductance absorbs energy. On discharge, the inductance releases energy. If the capacitance is sufficiently large, a stable electric current can be maintained during the discharge process in the output terminal. If this on and off process continuously repeats, the voltage in both sides of capacitance is higher than the input voltage. This adjustment, which involves changes in the battery power, is an effective control method, as shown in Fig. 9. Owing to the maximum power control structure, a PV cell can approach or reach the MPO in different environments. Among them, I_{pv} and U_{pv} are two output variables during the PV grid-connected process.

The INC method was used for MPPT control. Instantaneous conductivity changes in the PV array can be monitored, and the MPP can be defined. The PV cell conductivity changes with the MPP, which corresponds to the

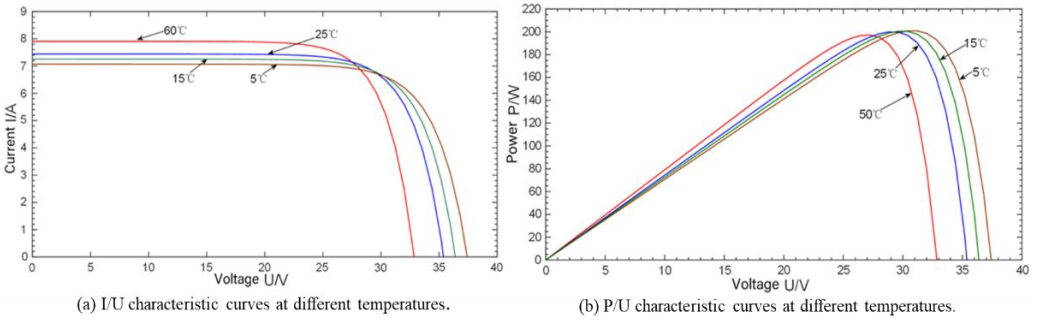

(a) I/U characteristic curves at different temperatures. (b) P/U characteristic curves at different temperatures.

Fig. 8: I/U (a) and P/U (b) characteristic curves of different temperatures at a constant temperature.

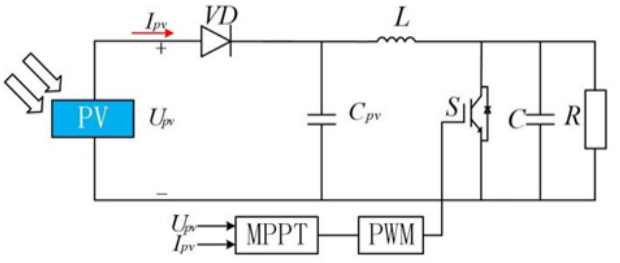

Fig. 9: Maximum output algorithm control structure.

point at which the conductivity changes significantly. In this study, MPPT realization by INC steps were as follows:

(1) The voltage (U) and power (P) of the PV cell were measured.
(2) The rate of change in the conductivity (G) was calculated as dG/dV.
(3) The MPP was confirmed when dG/dV=0.

With this method, additional sensors and complicated mathematical models are not required. The MPPT can be found only with voltage and current measurements. Additionally, the INC algorithm is robust to the nonideal characteristics of PV cells and environmental changes. A comparison of the advantages and limitations of INC with other MPPT methods is shown in Table 3.[32]

Table 3: Comparison of the advantages and limitations of INC with other MPPT methods.

Method	Advantages	Limitations
Perturbation and observation (P&O)	(1) Simple implementation (2) Low hardware cost (3) A priori knowledge of the PV array not required	(1) Oscillation occurs in a rapidly changing illumination (2) Low steady-state efficiency (3) Step selection proceeds sensitively
Fuzzy logic control (FLC)	(1) Adapted to nonlinear environment (2) Strong noise immunity (3) Accurate mathematical model not required	(1) Complex design (2) Computing resource requirements are too high (3) Difficult to adjust parameters
Artificial neural network (ANN)	(1) Adapted to complex environment model (2) High predictive ability (3) Strong adaptability	(1) Too much training data (2) High hardware implementation coat (3) Overfitting risk
Particle swarm optimization (PSO)	(1) Strong global search ability (2) Adapted to multi-peak MPPT	(1) High computational cost (2) Complex parameter optimization (3) Slow convergence
INC	(1) Fast dynamic response (2) High steady-state accuracy (3) Low oscillation	(1) High computation complexity (2) Sensitive to sensor noise (3) Higher precision voltage and current sampling requirements

As shown in Fig. 10, the operating points were continuously adjusted using the INC algorithm. The PV cell always operated around the MPPT. This method can significantly improve the energy utilization of PV systems, from which solar energy can be maximally used. Based on accurate control and optimization, MPPT technology plays an important role in the field of PV power generation.

The control process of the INC algorithm is shown in Fig. 11.

In Fig. 11, the duty cycle variation is ΔD. The MPP is defined as the change in dG/dV. In MPPT, the value of dG/dV changed from positive to negative. The duty cycle was adjusted to search for the MPP. This is a function of tracking control. In Figure 11, V(k) and I(k) represent the latest detected voltages and currents, respectively; and V(k-1) and I(k-1) are the previous detected voltage and current, respectively. The D-values of the latest and previously detected values were calculated. K is a variable coefficient with a value in the range of 5-10.

Regarding the illumination mutation condition, the INC Lyapunov stability analysis steps were as follows:

(1) System modeling:
The PV system dynamic equation (continuous-time) is as Eq. 12:

$$\begin{cases} \dot{V} = u \\ \dfrac{dI}{dV} \approx \dfrac{\Delta I}{\Delta V} \end{cases} \tag{12}$$

where u is the control input (duty cycle adjustment), V is the PV output voltage, and I is the output current.

(2) Considering the power error $e = \frac{dP}{dV}$ (MPP criterion), the Lyapunov function is as Eq. 13:

$$e = \frac{dP}{dV} = I + V\frac{dI}{dV} \tag{13}$$

(3) The piecewise Lyapunov function was constructed. If illumination mutation occurred, $\dot{V}(e) < 0$ prompted $e \to 0$ (converge to MPP) as Eq. 14:

$$V(e) = \frac{1}{2}e^2 > 0(\forall e \neq 0) \tag{14}$$

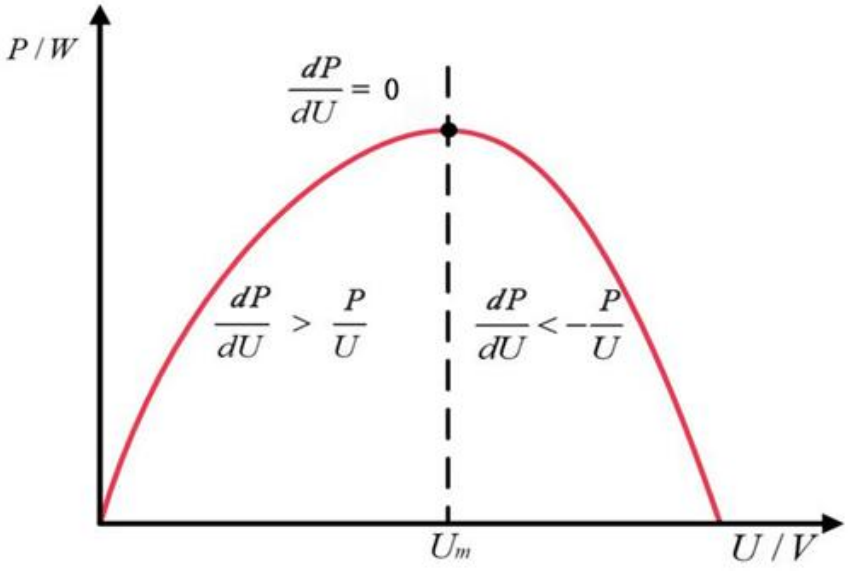

Fig. 10: Operation principle of the INC method.

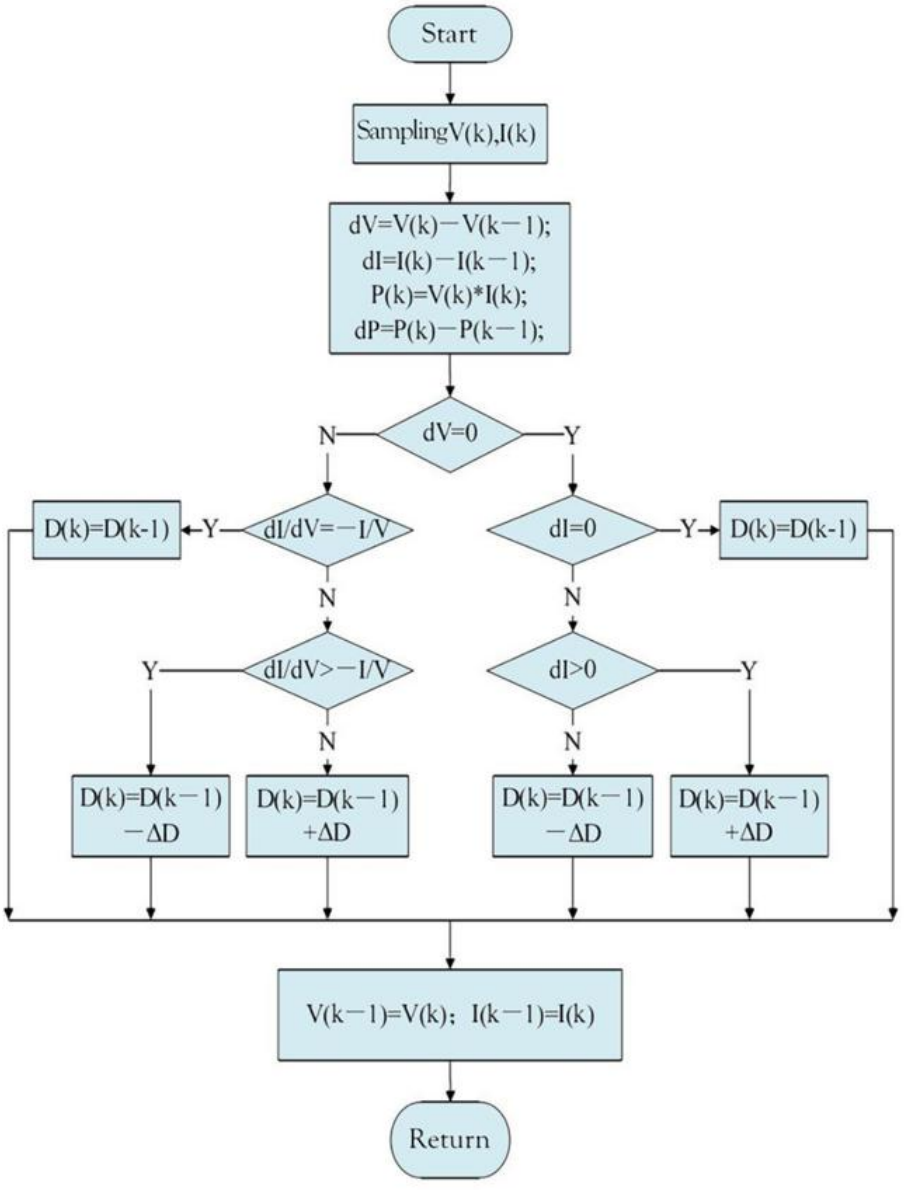

Fig. 11: INC algorithm control flow.

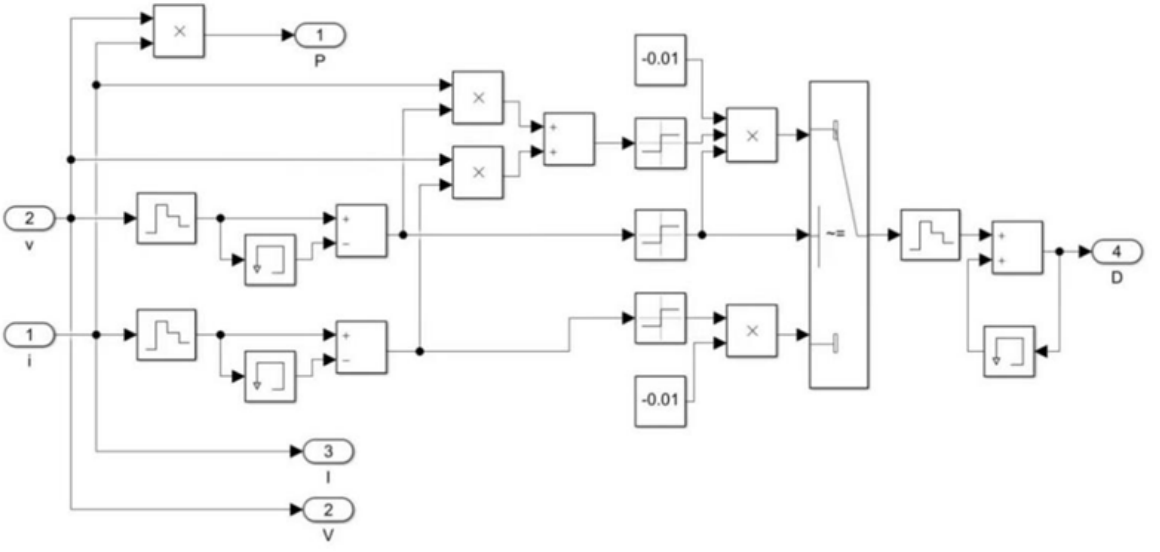

Fig. 12: INC simulation module.

4. Simulation of different influence factors on the output power

Based on the output characteristics of the PV cell, the MPO of the PV array was affected by the MPPT algorithm, light intensity, and temperature. Therefore, a wide-range and fast-response INC algorithm was used as the MPPT control algorithm.

4.1 MPPT controller

The MPPT controller is the core component of a PV power generation system realizing MPPT. The main function of this module is using the relevant MPPT algorithm to adjust the duty cycle of the boost circuit, from which the boost circuit can be driven by the PWM output signal. Therefore, this module should include an MPPT algorithm and implement PWM.

The simulation module is shown in Fig. 12. It uses the INC method to realize PWM control. As the MPPT control algorithm, the INC method has high precision and is easy to implement. The implementation principle of the INC method is as follows: The V-P curve of the PV cell in Fig. 8 shows that $dP/dU = 0$ at the MPP. According to mathematical derivation, at the MPP, $dI/dU = -I/U$ is valid. Therefore, when the output conductivity variation of the PV cell ($dG = dI/dU$) is equal to the negative value of the output conductance ($G = I/U$), the solar battery operates at the MPP. Therefore, $G + dG$ can be used to identify whether the PV power generation system operates at the MPP. If $G + dG < 0$, the system operates on the right side of the MPP. At this point, the output voltage should be reduced. If $G + dG > 0$, the system operates on the left side of the MPP. At this point, the output voltage should be increased. Only if $G + dG = 0$ does the system operate at the MPP.

The control structure of the duty cycle is shown in Fig. 13.

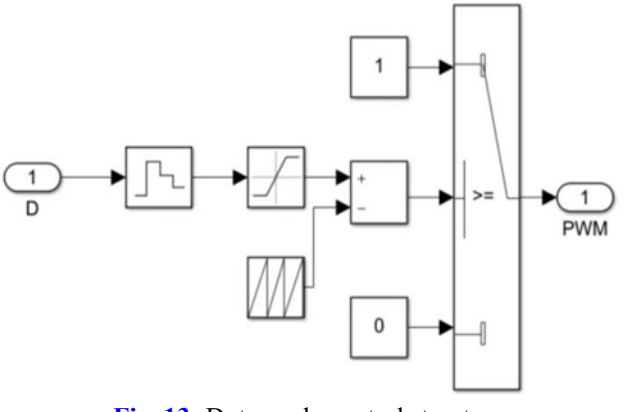

Fig. 13: Duty cycle control structure.

4.2 Effect of different light intensities on the output power

The constant temperature and initial light intensity were set at 25 °C and 1000 W/m^2, respectively. The light intensity at 1 s fluctuated at 500 W/m^2 and increased to 800 W/m^2 after 2 s. The PV panel parameters are listed in Table 4, and the temperature and light intensity curves are shown in Fig. 14.

Table 4: PV panel parameters.

Parameter	Value
Short-circuit current/I_{sc}	8.35 A
OCV/U_{sc}	43.6 V
MPP voltage/U_m	34.5 V
MPP current/I_m	7.5 A
MPP power/P_m	258.75 W

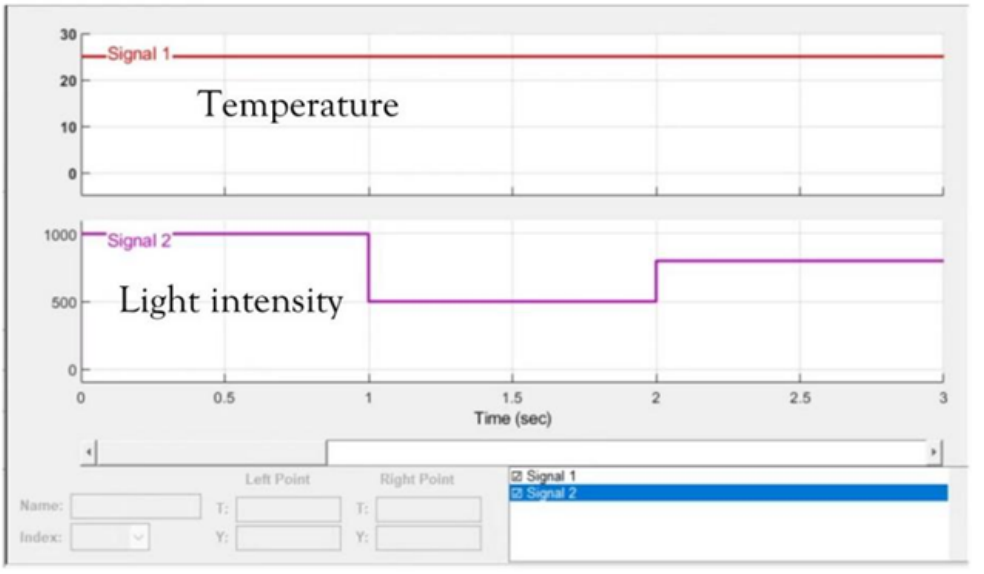

Fig. 14: Temperature (constant) and light intensity (variable) curves.

As shown in Fig. 15(a), the PV output voltage fluctuated at approximately 34.5 V within 0.12 s. Although the light intensity changed, the voltage fluctuation remained small. As shown in Fig. 15(b), during the initial stage of the simulation, the output current rapidly reached 7.5 A, which aligns with the initial PV panel setup parameters. The current waveform can be clearly observed according to the partial enlargement of the oscilloscope. However, with changes in light intensity, the fluctuation became more pronounced. According to the PV output curve shown in Fig. 15(c), the incremental conductance was flexibly adjusted. Within 0.12 s, the MPP was rapidly tracked, which output the power. With changes in light intensity, the MPPT control algorithm continued to adjust, identifying the MPP.

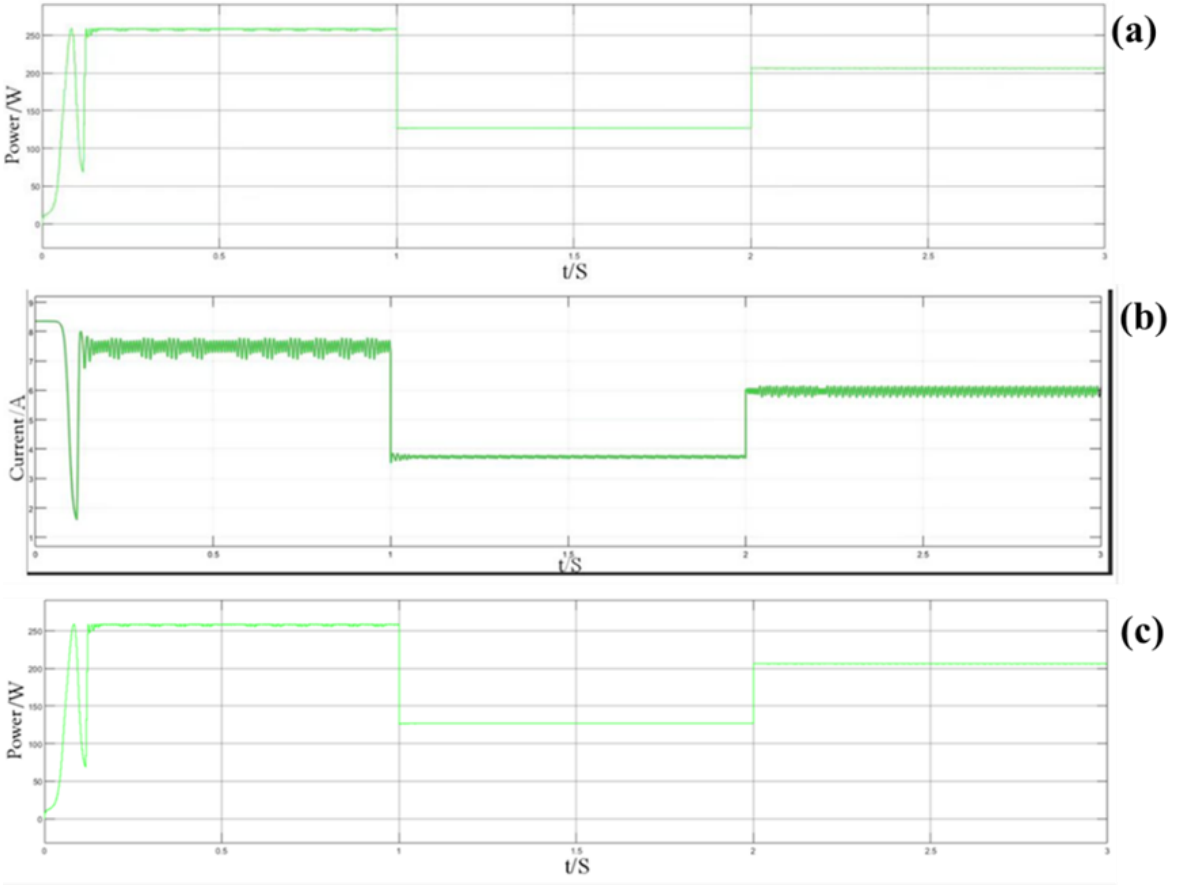

Fig. 15: PV array output curves under different light intensities. (a) Output voltage/V, (b) Output current/A, and (c) Maximum power output (W).

To enhance the robustness of MPPT, a fuzzy logic observer (FLO)-MPPT controller was used to prove the stability of the algorithm, using the following steps:
(1) The error variables were defined as Eq. 15:

$$e = P_{pv} - P_{MPP}, \Delta e = \frac{de}{dt} \tag{15}$$

(2) The Lyapunov function was constructed as Eq. 16:

$$V(e) = \frac{1}{2}e^2 > 0(\forall e \neq 0) \tag{16}$$

(3) Fuzzy control rate design:
Input: e and Δe → Fuzzification → Fuzzy rule base → Defuzzification → Output u (duty cycle increment ΔD)
(4) Lyapunov optimization constraint:
The control rate was governed by Eq. 17:

$$\dot{V} = e \cdot \dot{e} \leq -\kappa e^2 \tag{17}$$

The PV system model $\dot{e} = f(e, u, d)$ was substituted, from which the stable domain of u was determined.

4.3 Effect of different temperatures on the power output

The light intensity was set to 1000 W/m^2 and the initial temperature was set to 25 ℃. The temperature increased to 35 ℃ in 1 s and decreased to 30 ℃ in 1.5 s thereafter. In 2.5 s, the temperature decreased again to 25 ℃. The PV panel parameters are listed in Table 2 and the temperature and light intensity curves are shown in Fig. 16.

The effects of different temperatures on the PV array power output results are shown in Fig. 17, including the actual output voltage and current.

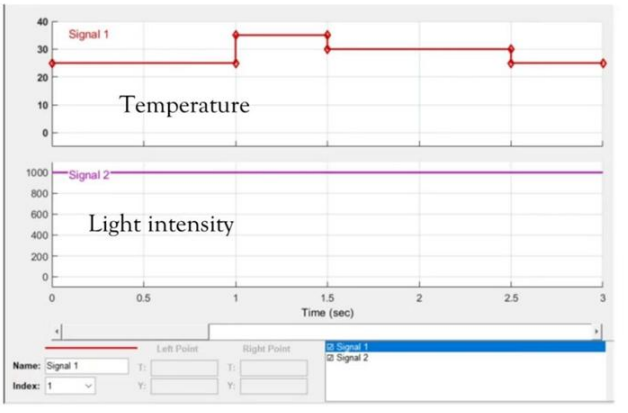

Fig. 16: Temperature (variable) and light intensity (constant) curves.

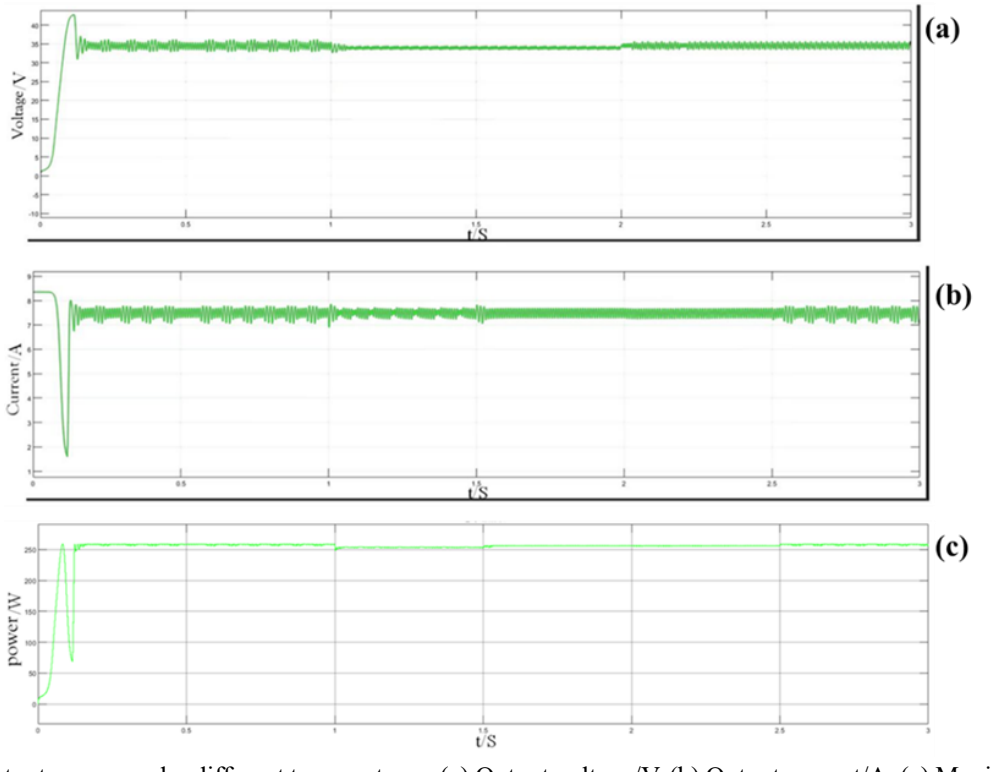

Fig. 17: PV array output curves under different temperatures. (a) Output voltage/V, (b) Output current/A, (c) Maximum power output (W).

From Fig. 17(a), in 0.16 s, the PV output voltage fluctuated by approximately 34.5 V. Although the temperature changed, the voltage fluctuation was minimal.

As shown in Fig. 17(b), in the initial stage of the simulation, the output current quickly reaches 7.5 A, which aligns with the initial PV panel setup parameters. The current waveform can be clearly observed according to the partial enlargement of the oscilloscope. However, with changes in temperature, the current change is insignificant. According to the PV output curve shown in Fig. 17(c), the incremental conductance is flexibly adjusted. In 0.16 s, the MPPT is quickly tracked, which outputs power. The maximum power output did not change with changes in temperature.

Overall, the primary factors affecting the maximum power output are light intensity changes and the MPPT algorithm, with the effect of light intensity being the most significant. According to the controlled experiment, the power prediction trend conformed to the output characteristics of the PV cell. The simulation data is consistent with manufacturers' datasheets.

5. Conclusion

With rapid socioeconomic development, traditional energy-supplying modes cannot meet the demand for overall growth. PV energy, a renewable and clean energy source, holds wide application prospects. Based on the references, the environmental factors make great effect on output characteristics of photovoltaic system. The solar irradiance and temperature are mainly influence factors. According to the meteorological data under different weather condition, the photovoltaic system output can be calculated by Matlab simulation model. It makes positive effect on power grid dispatch. In this manuscript, from the changes of PV system output characteristic curve with meteorological data changing, the meteorological parameters in simulation model is adjusted to acquire higher output power. It is consistent with real experimental result. Based on the output characteristics of photovoltaic system under different typical day, the temperature range of solar panels can be roughly found. It can prevent the thermal damage. The working status of photovoltaic system can be real-time tested. According to the regular cleaning, maintenance and overhaul for solar panels, the service life of solar panels will be extended. Besides, the output power of photovoltaic system can be stabilized, which improves the working efficiency of photovoltaic system. According to the deployment analysis of the PV power generation theory, the following conclusions can be drawn:

(1) The working characteristics and principles of the PV supply were analyzed, exploring the characteristics and advantages of the PV supply. According to an analysis of PV microgrid construction object, the incremental conductance was used for power planning.

(2) PV cells in the microgrid were modeled using the PV cell module in Simulink, and the DC load module was modeled using the RLC load in an electrical storehouse. Subsequently, the simulation parameters were defined.

(3) The output characteristics of the PV power supply and output were simulated. Test results showed that with increasing temperature, system output power and voltage declined, and vice vera. Thus, temperature changes are inversely proportional to the output characteristics of PV power generation, although, the effect was minimal.

(4) The effect of light intensity on the PV power generation output characteristics was significant. When light intensity significantly changed (from 1000 w/m^2 to 600 w/m^2), the output power of the PV system became unstable. This observation suggested that the performance of the PV system was poor under weak light intensities. Thus, a DC boost circuit can improve output stability.

In this research, one kind of nonlinear system optimization based on derivative is developed, which can be extended to non-convex optimization problem with PV characteristics kind (Such as fuel cell and chemical reaction process). The proposed work in future work is as follows:

From the experimental result, the MPPT control system in this manuscript can be used for simulation research of MPPT in PV power generation system. It is very significant for the research of external environment effect on PV power generation control. Meanwhile, the pure inductive loads are selected in Boost simulation circuit. Regarding to the effect of capacitive reactance loads on MPPT control system, it is still needed for further research.

Acknowledgments

This research was aided by the key area campaign of regular universities in Guangdong province (Nos. 2021ZDZX1058 and 2024ZDZX4074), Guangdong Basic and Applied Basic Research Foundation (Nos. 2025A1515010595 and 2023A1515240063).

Conflict of Interest

The authors declare no conflict of interest.

Use of AI tools declaration

The authors declare they have not used Artificial Intelligence (AI) tools in the creation of this article.

Supporting Information

Not applicable.

CRediT Statement

Guang Yu: Writing - Review and editing, Supervision, Resources, Project administration, Investigation, Software. **Lijie Peng:** Writing - Original draft, Methodology, Investigation, Formal analysis, Data curation. **Yujia Cheng**:

Writing - Review and editing, Funding acquisition.

References

[1] J. B. Dias, S. Bator, P. Poggi, B. Ferrari, Hybrid microgrid simulation, *Journal of Solar Energy Engineering*, 2016, **138**, 044501, doi: 10.1115/1.4033404.

[2] E. Jacob, H. Farzaneh, Dynamic modeling and experimental validation of a standalone hybrid microgrid system in Fukuoka, Japan, *Energy Conversion and Management*, 2022, **274**, 116462, doi: 10.1016/j.enconman.2022.116462.

[3] N. Gupta, B. R. Prusty, Probabilistic load flow of an islanded microgrid with WTGS and PV uncertainties containing electric vehicle charging loads, *International Transactions on Electrical Energy Systems*, 2022, **2022**, 9569224, doi: 10.1155/2022/9569224.

[4] M. Simonazzi, N. Delmonte, P. Cova, R. Menozzi, Models for MATLAB simulation of a university campus micro-grid, *Energies*, 2023, **16**, 5884, doi: 10.3390/en16165884.

[5] V. K. Dunna, K. P. B. Chandra, P. K. Rout, B. K. Sahu, Design and real-time validation of higher order sliding mode observer-based integral sliding mode MPPT control for a DC microgrid, *IEEE Canadian Journal of Electrical and Computer Engineering*, 2022, **45**, 418-425, doi: 10.1109/ICJECE.2022.3211470.

[6] Y. Tang, Q. Xun, M. Liserre, H. Yang, Energy management of electric-hydrogen hybrid energy storage systems in photovoltaic microgrids, *International Journal of Hydrogen Energy*, 2024, **80**, 1-10, doi: 10.1016/j.ijhydene.2024.07.017.

[7] J. Gu, L. Xie, X. Yang, Y. Zhang, L. Wang, Q. Wang, W. Zhang, B. Wang, Fuzzy piecewise coordinated control and stability analysis of the photovoltaic-storage direct current microgrid, *IET Renewable Power Generation*, 2022, **16**, 3311-3324, doi: 10.1049/rpg2.12584.

[8] Y. V. Garcia, O. Garzon, F. Andrade, A. Irizarry, O. F. Rodriguez-Martinez, Methodology to implement a microgrid in a university campus, *Applied Sciences*, 2022, **12**, 4563, doi: 10.3390/app12094563.

[9] X. Meng, Z. Liu, Y. Liu, H. Zhou, I. A. Tasiu, B. Lu, J. Gou, J. Liu, Conversion and SISO equivalence of impedance model of single-phase converter in electric multiple units, *IEEE Transactions on Transportation Electrification*, 2023, **9**, 1363-1378, doi: 10.1109/TTE.2022.3203006.

[10] P. K. Kesavan, U. Subramaniam, D. J. Almakhles, S. Selvam, Modelling and coordinated control of grid connected photovoltaic, wind turbine driven PMSG, and energy storage device for a hybrid DC/AC microgrid, *Protection and Control of Modern Power Systems*, 2024, **9**, 154-167, doi: 10.23919/PCMP.2023.000272.

[11] X. Wang, C. Q. Jiang, J. Zhou, L. Mo, Y. Wang, Enhanced modeling of wireless power transfer system with battery load, *IEEE Transactions on Power Electronics*, 2024, **39**, 6574-6579, doi: 10.1109/TPEL.2024.3367920.

[12] M. Shaban, I. Ben Dhaou, M. F. Alsharekh, M. Abdel-Akher, Design of a partially grid-connected photovoltaic microgrid using IoT technology, *Applied Sciences*, 2021, **11**, 11651, doi: 10.3390/app112411651.

[13] J. Tang, J. Liu, J. Wu, G. Jin, H. Kang, Z. Zhang, N. Huang, RAC-GAN-based scenario generation for newly built wind farm, *Energies*, 2023, **16**, 2447, doi: 10.3390/en16052447.

[14] Z. B. Liu, X. J. Liu, Improved multi-hysteresis control strategy of hybrid storage system in a stand-alone DC microgrid, *Transactions of China Electrotechnical Society*, 2018, **33**, 490-497, doi: 10.19595/j.cnki.1000-6753.tces.161658.

[15] E. Ozturk, E. Ogliari, M. Sakwa, A. Dolara, N. Blasuttigh, A. M. Pavan, Photovoltaic modules fault detection, power output, and parameter estimation: a deep learning approach based on electroluminescence images, *Energy Conversion and Management*, 2024, **319**, 118866, doi: 10.1016/j.enconman.2024.118866.

[16] C. Álvarez-Arroyo, S. Vergine, A. S. de la Nieta, L. Alvarado-Barrios, G. D'Amico, Optimising microgrid energy management: Leveraging flexible storage systems and full integration of renewable energy sources, *Renewable Energy*, 2024, **229**, 120701, doi: 10.1016/j.renene.2024.120701.

[17] D. Naamane, H. Benbouhenni, A. Chebabhi, Z. Laid, D. Zellouma, I. Colak, A new nonlinear control to improve the efficiency of the PV-SAPF system, *Energy Reports*, 2024, **11**, 3096-3116, doi: 10.1016/j.egyr.2024.02.051.

[18] S. Wang, X. Yuan, Q. Huang, A. Chen, H. Ma, X. Xu, Daily consumption monitoring method of photovoltaic microgrid based on genetic wavelet neural network, *International Journal of Low-Carbon Technologies*, 2023, **18**, 167-174, doi: 10.1093/ijlct/ctac141.

[19] Wenham, SR.; Green, MA.; Watt, ME.; Corkish, R.; Sproul, A. *PV System Analysis, Applied Photovoltaics[M]*, Routledge, London, 2011, 61-84, ISBN: 978-1-84407-401-6.

[20] H. He, N. Zhang, C. Kang, S. Ci, F. Teng, G. Strbac, Communication resources allocation for time delay reduction of frequency regulation service in high renewable penetrated power system, *CSEE Journal of Power and Energy Systems*, 2024, **10**, 468-480.

[21] W. Wang, C. Li, Y. He, H. Bai, K. Jia, Z. Kong, Enhancement of household photovoltaic consumption potential in village microgrid considering electric vehicles scheduling and energy storage system configuration, *Energy*, 2024, **311**, 133330, doi: 10.1016/j.energy.2024.133330.

[22] J. Lou, H. Cao, X. Meng, Y. Wang, J. Wang, L. Chen, L. Sun, M. Wang, Power load analysis and configuration optimization of solar thermal-PV hybrid microgrid based on building, *Energy*, 2024, **289**, 129963, doi: 10.1016/j.energy.2023.129963.

[23] Green, MA. The Limits, Losses, and Measurement of Efficiency, *Silicon Solar Cells Advanced Principles & Practice[M]*, Shanghai Jiao Tong University, Press, Shanghai, 2010, 50-90, ISBN: 9787313061911.

[24] M. B. Sene, A. Samoura, S. Diouf, A. Diao, C. Mbow, Electrical modeling of a silicon photovoltaic solar cell: comparative study of models characterizing the photovoltaic solar cell, *Open Journal of Applied Sciences*, 2023, **13**, 1787-1795, doi: 10.4236/ojapps.2023.1310141.

[25] H. Wang, X. Wu, K. Sun, X. Du, Y. He, K. Li, Economic dispatch optimization of a microgrid with wind–photovoltaic-load-storage in multiple scenarios, *Energies*, 2023, **16**, 3955,

doi: 10.3390/en16093955.
[26] J. Lou, Y. Wang, H. Wang, J. Wang, L. Chen, J. Zhang, M. R. Islam, K. J. Chua, Operation characteristics analysis and optimal dispatch of solar thermal-photovoltaic hybrid microgrid for building, *Energy and Buildings*, 2024, **315**, 114340, doi: 10.1016/j.enbuild.2024.114340.
[27] Z. Weng, J. Zhou, Z. Zhan, Reliability evaluation of standalone microgrid based on sequential Monte Carlo simulation method, *Energies*, 2022, **15**, 6706, doi: 10.3390/en15186706.
[28] X. Pei, X. Zhao, H. Jia, H. Wang, J. Liu, Fuzzy sliding mode control with adaptive exponential reaching law for inverters in the photovoltaic microgrid, *Frontiers in Energy Research*, 2024, **12**, 1416863, doi: 10.3389/fenrg.2024.1416863.
[29] E. Szilagyi, D. Petreus, M. Paulescu, T. Patarau, S.-M. Hategan, N. A. Sarbu, Cost-effective energy management of an islanded microgrid, *Energy Reports*, 2023, **10**, 4516-4537, doi: 10.1016/j.egyr.2023.10.088.
[30] C. Nan, Y. Hao, X. Huang, H. Wang, H. Yang, Investigation on temperature dependence of recent high-efficiency silicon solar modules, *Solar Energy Materials and Solar Cells*, 2024, **266**, 112649, doi: 10.1016/j.solmat.2023.112649.
[31] M. AlMuhaini, A. Yahaya, A. AlAhmed, Distributed generation and load modeling in microgrids, *Sustainability*, 2023, **15**, 4831, doi: 10.3390/su15064831.
[32] M. H. Ali, M. Zakaria, S. El-Tawab, A comprehensive study of recent maximum power point tracking techniques for photovoltaic systems, *Scientific Reports*, 2025, **15**, 14269, doi: 10.1038/s41598-025-96247-5.